 CMES, vol.29, no.3, pp.151-162, 2008

The Geometric Interpretation of Linking Number, Writhe and Twist for a Ribbon

C. K. Au[1]

Abstract: Ribbons may be used for the modeling of DNAs and proteins. The topology of a ribbon can be described by the linking number, while its geometry is represented by the writhe and the twist. These quantities are integrals and are related by the Călugăreanu's theorem from knot theory. This theorem also describes the relationship between the various conformations. The heart of the Călugăreanu's theorem rests in the Gauss Integral. Due to the large number of molecules, the topology and the geometry of a ribbon model can be very complicated. As a result, these integrals are commonly evaluated by numerical methods. The writhe of a ribbon is usually computed by mapping its self-crossing onto a unit sphere. The twist of a ribbon is mainly due to the geometric relationship between its central spine and boundary. This article offers a geometric interpretation of the twist of a ribbon in terms of crossing between the central spine and boundary of the ribbon. This approach facilitates the calculation of the twist of a ribbon. Some basics in visibility will enhance the intuition.

Keyword: Linking number, writhe, twist, Gauss Integral, Călugăreanu's theorem.

1 Introduction

Coiling and twisting are common physical phenomena of filament deformation. It can be found in example from everyday life such as ribbon and telephone cords as well as the nano-scale DNA [Steffen, Murphy, Lathrop, Opel, Tolleri and Hatfield (2002)] and protein molecules [Karcher, Lee, Kaazempur-Mofrad and Kamm (2006)], and carbon nanotube [Park, Cho, Kim, Jun and Im (2006)]. Bending due to applied forces in straight carbon nanotube can be easily happen while intrinsically coiled tubes have been observed as well. A curve has only length; it has no width or thickness. If endowed with a width in a certain direction, a curve becomes a *ribbon*. If the width is uniform in all directions, then a *tube* results. Ribbons serve as a convenient way to model macromolecules such as DNA and protein [Carson and Bugg (1986), (1987), (2000)]. The functions of these macromolecules are determined by their form, or *geometry*, while their inter-connectedness, or *topology*, is important to many biological processes [Cozarelli, Boles and White (1990), Fuller (1971)] such as protein folding, replication and transcription. In the parlance of biology, the chemical constituents, in a linear string of symbols, are called the "primary" representation. The spatial arrangement of balls-and-sticks, as in the celebrated double-helix model for the DNA, is called the "secondary" representation. Upon a closer examination, the balls at the two ends of a stick follow certain geometric motifs.

Thus, the two helical clusters of amino acids in the DNA, for example, can be abstracted as two intertwining ribbons.

Curvature and torsion characterize how a curve **L** changes with respect to the Frenet-Serret frame on the curve itself. But suppose the frame of reference is on another curve **K**. Then, two new quantities, *writhe* and *twist*, arise. In a closed end ribbon, let there be a central "spine" **K**. Also, let one of the two boundary curves of the ribbon be **L**. Then, the "tangling" between curve **K** and curve **L** gives an indication of how complex the ribbon is, spatially. Intuitively, as writhe and twist are analogous to curvature and torsion, they describe the geometry of a ribbon. Yet, because curve **K**

[1] School of Mechanical and Aerospace Engineering, Nanyang Technological University, Singapore. Email: mckau@ntu.edu.sg

"threads" curve **L**, or vice versa, there must be another parameter that characterizes the "knottiness" of the tangle – called *linking number*, a topological quantity. Indeed, the Călugăreanu's theorem [Călugăreanu's (1959)] gives the connection.

The topology of two separate curves (of zero width and thickness) is easier to visualize than that of a single ribbon (with one curve as its "spine" and another as its boundary). Consider the two interlocking closed end curves **K** and **L**, the linking number $Lk(\mathbf{K},\mathbf{L})$ remains the same even more geometry is added to the two curves – by giving each more writhe and twist. For two open end curves, their linking number would necessarily be $Lk(\mathbf{K},\mathbf{L}) = 0$, as one can "slip" out of the entanglement by the other. Similarly, for two curves, one closed and the other open, the linking number $Lk(\mathbf{K},\mathbf{L}) = 0$; they are not linked.

Fundamentally, the two quantities, linking number $Lk(\mathbf{K},\mathbf{L})$ and writhe $Wr(\mathbf{K},\mathbf{K})$ are rooted in the evaluation of the so-called *Gauss Integral*. Due to the large number of molecules, the topology and the geometry of a ribbon model can be very complicated. As a result, difficulties arise in evaluating the integral. Several approaches for computing the writhe of a polygonal curve [Banchoff (1976), Cimasoni (2001), Agarwal, Edelsbrunner and Wang (2002), Dennis and Hannay (2005), Klenin and Langowski (2000)] are discussed. Different from the evaluation of writhe and linking number of a ribbon which only involve the ribbon central spine and boundary, computation of twist of a ribbon needs to consider the material between two curves. This paper reviews the technique of interpreting the writhe in terms of spherical area and offers a similar geometric interpretation to the twist which enables an approximation formula. Based on these interpretations, it also explains the algebraic property of summing up two real numbers of writhe and twist always yields a linking number integer in the Cãlugãreanu's theorm.

2 Reviews

Mathematically, the linking number $Lk(\mathbf{K},\mathbf{L})$ [Dennis and Hannay (2005)] between two closed end space curves **K** and **L** is given by

$$Lk(\mathbf{K},\mathbf{L}) = \frac{1}{4\pi} \oint\!\!\oint_{\mathbf{K}\times\mathbf{L}} \frac{(d\mathbf{p}\times d\mathbf{q})\cdot\mathbf{pq}}{|\mathbf{pq}|^3} \tag{1}$$

Similarly, the writhe $Wr(\mathbf{K},\mathbf{K})$ [Dennis and Hannay (2005)] of a closed end curve **K** is

$$Wr(\mathbf{K},\mathbf{K}) = \frac{1}{4\pi} \oint\!\!\oint_{\mathbf{K}\times\mathbf{K}} \frac{(d\mathbf{p}\times d\mathbf{q})\cdot\mathbf{pq}}{|\mathbf{pq}|^3} \tag{2}$$

where the expression $\oint\!\!\oint_{\mathbf{K}\times\mathbf{L}} \frac{(d\mathbf{p}\times d\mathbf{q})\cdot\mathbf{pq}}{|\mathbf{pq}|^3}$ is termed Gauss Integral.

2.1 Crossing number as complex measure

The amount of entanglement of two space curves can be characterized by the number of crossings. The intuition is clear: the more crossings there are, the more entangled the two curves must be in space. Yet, the number of crossings depends on the direction of the projection. In other words, over all possible orientations, there must be a direction which gives the maximal number of crossings; corresponding, there must be one that yields the minimal. *A weighted average with crossing number as the weight over all angles can be calculated.*

The crossing of two space curves is determined by the *visibility*. A point **q** is visible to point **p** if there is *a line of sight* **pq** connecting the points **p** and **q**. Two space curves *cross* each other if a point on one curve is visible to a point on the other curve.

Consider two space curve segments, $d\mathbf{q}$ and $d\mathbf{p}$, a point **p** on segment $d\mathbf{p}$, as the source for viewing the target segment $d\mathbf{q}$. As the point **p** moves along segment $d\mathbf{p}$, segment $d\mathbf{q}$ is visible to point **p** if the line of sight **pq** intersects the planar quadrilateral area $dA = \frac{(d\mathbf{p}\times d\mathbf{q})\cdot\mathbf{pq}}{|\mathbf{pq}|}$ which is perpendicular to the line of sight **pq** as depicted in figure 1. The *solid angle* $d\Omega$ includes all lines of sight along which the segment $d\mathbf{q}$ crosses $d\mathbf{p}$ is given by

$$d\Omega = \frac{dA}{|\mathbf{pq}|^2} = \frac{(d\mathbf{p}\times d\mathbf{q})\cdot\mathbf{pq}}{|\mathbf{pq}|^3} \tag{3}$$

Hence, the solid angle equals to the Gauss Integral.

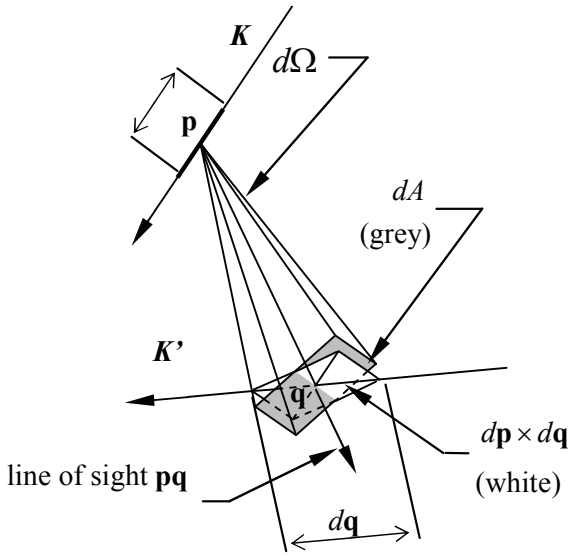

Figure 1: Planar quadrilateral and solid angle

When two curves are oriented, in having a "head" and a "tail", then the notion of *signed crossing* arises due to the cross product $d\mathbf{p} \times d\mathbf{q}$ in the planar quadrilateral dA. Given two skewed curve segments $d\mathbf{q}$ and $d\mathbf{p}$, the crossing is said to be *positive*, if the tip of the arrow for the curve segment in front (ordered along the direction of line of sight, from the source to the view plane) is to be rotated counter-clockwise with an angle less than π – in order to be aligned with the curve segment in the back; conversely, the crossing is *negative*.

Mapping the solid angle in equation (3) onto a unit sphere is a common approach to evaluate the Gauss Integral.

Definition A *crossing map* χ_K is a map of the line of sight from curve segment $\mathbf{K}$ to $\mathbf{L}$ on a unit sphere $\mathbf{S}$ (these two curve segments $\mathbf{K}$ and $\mathbf{L}$ can be either from a single curve or two distinct curves), hence $\chi_K : \mathbf{K} \times \mathbf{L} \rightarrow \mathbf{S}$such that $\mathbf{v} = \chi(\mathbf{p},\mathbf{q}) = \frac{\mathbf{pq}}{|\mathbf{pq}|}$, $\forall \mathbf{p} \in \mathbf{K}$, $\forall \mathbf{q} \in \mathbf{L}$ and $\mathbf{v} \in \mathbf{S}$.

Figure 2 shows the relationship between the signed area of the planar quadrilateral dA (as depicted in figure 2) and that of the spherical quadrilateral dS on a unit sphere $\mathbf{S}$. Since both areas dS and dA subtend the same solid angle $d\Omega$ in a sphere:

$$d\Omega = \frac{dA}{|\mathbf{pq}|^2} = \frac{dS}{r^2} \tag{4}$$

where $r = 1$ is the radius of the unit sphere.

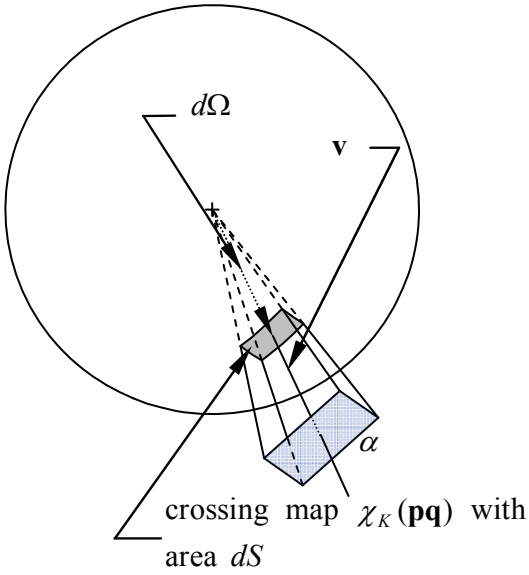

Figure 2: Spherical quadrilateral and planar quadrilateral

2.2 Computation of linking number and writhe

The linking number $Lk(\mathbf{K},\mathbf{L})$ between the two curve segments $\mathbf{K}$ and $\mathbf{L}$ is the average value of the signed crossing number over every possible line of sight:

$$Lk(\mathbf{K},\mathbf{L}) = \frac{1}{4\pi}\int d\Omega \tag{5}$$

which yields the expression as defined by equation (1). Similarly, the writhe $Wr(\mathbf{K},\mathbf{K})$ of a self intersect curve $\mathbf{K}$ is the average value of the signed crossing number over every possible line of sight:

$$Wr(\mathbf{K},\mathbf{K}) = \frac{1}{4\pi}\int d\Omega \tag{6}$$

which gives equation (2) for the writhe $Wr(\mathbf{K},\mathbf{K})$.

Discretizing a curve into a series of line segments facilitates the computation of Gauss Integral numerically. Figure 3(a) shows two linear segments $\mathbf{p}_j\mathbf{p}_{j+1}$ and $\mathbf{q}_k\mathbf{q}_{k+1}$. The segments cross each other along the line of sight $\mathbf{pq}$.

Specifically, the point $\mathbf{p}$ can move along the segment $\mathbf{p}_j\mathbf{p}_{j+1}$ while the point $\mathbf{q}$ goes from $\mathbf{q}_k$ to

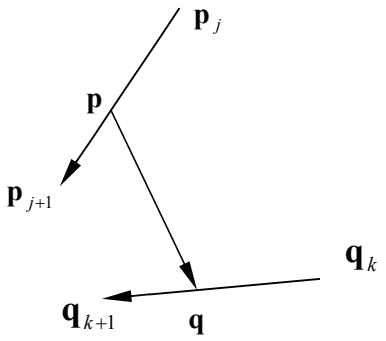

(a) Two linear segments

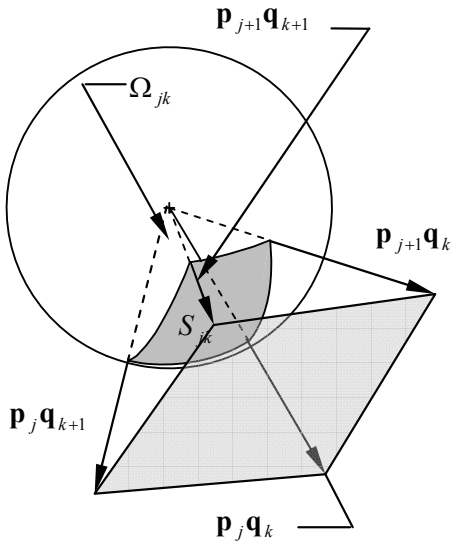

(b) The crossing

Figure 3: Angle ranges as curved quadrilateral

$\mathbf{q}_{k+1}$. The extreme solid angle Ω_{jk} of an area swept out on the unit sphere must be bounded by the four segments: $\mathbf{p}_j\mathbf{q}_k$, $\mathbf{p}_j\mathbf{q}_{k+1}$, $\mathbf{p}_{j+1}\mathbf{q}_k$ and $\mathbf{p}_{j+1}\mathbf{q}_{k+1}$.

The spherical quadrilateral crossing map with surface area S_{jk}, illustrated in figure 3(b), gives the entire range of solid angle Ω_{jk} along which the two line segments cross when projected.

From equation (3) and (4),

$$S_{jk} = \Omega_{jk} = \int_{\mathbf{p}_j}^{\mathbf{p}_{j+1}} \int_{\mathbf{q}_k}^{\mathbf{q}_{k+1}} \frac{(d\mathbf{p} \times d\mathbf{q}) \cdot \mathbf{pq}}{|\mathbf{pq}|^3} \tag{7}$$

where $\mathbf{p}_j \in \mathbf{K}$ and $\mathbf{q}_k \in \mathbf{L}$. Hence, the linking number given by equation (1) can be rewritten as

$$Lk(\mathbf{K},\mathbf{L}) = \frac{1}{4\pi} \sum_{\substack{j=1, \\ n+1=1}}^{n} \sum_{\substack{k=1, \\ n+1=1}}^{n} S_{jk}^{Lk} \tag{8}$$

where $S_{jk}^{Lk} = S_{jk}$, $\forall \mathbf{p}_j \in \mathbf{K}$, $\forall \mathbf{q}_k \in \mathbf{L}$.

Similarly, the writhe $Wr(\mathbf{K},\mathbf{K})$ expressed by equation (2) is rewritten as

$$Wr(\mathbf{K},\mathbf{K}) = \frac{1}{4\pi} \sum_{\substack{j=1 \\ j\neq k \\ j\neq k\pm 1 \\ n+1=1}}^{n} \sum_{\substack{k=1 \\ n+1=1}}^{n} \int_{p_j}^{p_{j+1}} \int_{q_k}^{q_{k+1}} \frac{(d\mathbf{p} \times d\mathbf{q}) \cdot \mathbf{pq}}{|\mathbf{pq}|^3} \tag{9}$$

which implies

$$Wr(\mathbf{K},\mathbf{K}) = \frac{1}{4\pi} \sum_{\substack{j=1 \\ j\neq k \\ j\neq k\pm 1 \\ n+1=1}}^{n} \sum_{\substack{k=1 \\ n+1=1}}^{n} S_{jk}^{Wr} \tag{10}$$

where $S_{jk}^{Wr} = S_{jk}$, $\forall \mathbf{p}_j \in \mathbf{K}$ and $\forall \mathbf{q}_k \in \mathbf{K}$.

Two special cases for the indices deserve some elaboration. When $j = k \pm 1$, the quadrilateral produced on the unit sphere is the great circle in the plane containing the two segments; its area is nil or $S_{jk} = 0$ $(j = k \pm 1)$. But when $j = k$, the area degenerates to a point (with zero area) on the unit sphere.

3 Computation of twist

The twist $Tw(\mathbf{K},\mathbf{L})$ of a ribbon is due to the *geometric relationship* between its central spine $\mathbf{K}$ and the boundary $\mathbf{L}$. Let $\mathbf{L}(s) = \mathbf{K}(s) + \mathbf{u}(s)$, where $\mathbf{u}(s)$ is a vector perpendicular to the unit tangent vector $\mathbf{t}$ of curve $\mathbf{K}$ pointing from curve $\mathbf{K}$ to curve $\mathbf{L}$ and s is their common parameter. The twist $Tw(\mathbf{K},\mathbf{L})$ [Dennis and Hannay (2005)] is

$$Tw(\mathbf{K},\mathbf{L}) = \frac{1}{2\pi} \int_{\mathbf{K}} (\mathbf{t} \times \mathbf{u}) \frac{d\mathbf{u}}{ds} \cdot ds \tag{11}$$

3.1 Twist of a ribbon

The computation of the twist $Tw(\mathbf{K},\mathbf{L})$ of a ribbon is different from that of its linking number

$Lk(\mathbf{K},\mathbf{L})$ and writhe $Wr(\mathbf{K},\mathbf{K})$, which only involve the curve $\mathbf{K}$ (the central spine of a ribbon) and curve $\mathbf{L}$ (one of the boundaries of a ribbon). Since the material between the central spine (curve $\mathbf{K}$) and the boundary (curve $\mathbf{L}$) also contribute to the twist, it must be considered in the computation.

A ribbon is characterized by two curves $\mathbf{K} = \mathbf{K}(s)$ and $\mathbf{L}(s) = \mathbf{K}(s) + \mathbf{u}(s)$ $(\forall s \in R)$ as shown in figure 4(a). Curve $\mathbf{K}$ represents the central spine of the ribbon while its boundary is the curve $\mathbf{L}$.

Let $\mathbf{K} = \mathbf{p}_1\mathbf{p}_2\cdots\mathbf{p}_n$ and $\mathbf{L} = \mathbf{q}_1\mathbf{q}_2\cdots\mathbf{q}_n$ be two series of line segments. A discrete ribbon model is shown in Figure 4(b) which relates all the points on curve $\mathbf{K}$ to those on curve $\mathbf{L}$. When the two free ends of the ribbon are connected into a closed knot, then $\mathbf{K} = \mathbf{p}_1\mathbf{p}_2\cdots\mathbf{p}_n\mathbf{p}_1$ and $\mathbf{L} = \mathbf{q}_1\mathbf{q}_2\cdots\mathbf{q}_n\mathbf{q}_1$.

In a discrete ribbon model, the integrals of linking number Lk and writhe Wr expressed in equation (1) and (2) can be computed more efficiently, and with nearly equal effectiveness, by considering their geometric meanings. A similar approach is employed to compute the twist Tw.

Rewriting equation (11) as

$$Tw(\mathbf{K},\mathbf{L}) = \sum_j Tw_j \tag{12}$$

with $Tw_j = \frac{1}{2\pi}\int_{\mathbf{p}_j}^{\mathbf{p}_{j+1}} (\mathbf{t}\times\mathbf{u})\frac{d\mathbf{u}}{ds}ds$. Consider the ribbon segment characterized by points $\mathbf{p}_j$, $\mathbf{p}_{j+1}$ on curve $\mathbf{K}$ as shown in figure 5. Since curve $\mathbf{K}$ and $\mathbf{L}$ have the same parmeterization, the corresponding points $\mathbf{q}_j$ and $\mathbf{q}_{j+1}$ are identified on curve $\mathbf{L}$. The segment $\mathbf{q}_j$ $\mathbf{q}_{j+1}$ twists around $\mathbf{p}_j$ $\mathbf{p}_{j+1}$ with dihedral angle α_j. Since the twist Tw in equation (11) can also been expressed in terms of crossings [13], the vectors $\mathbf{v}_1$, $\mathbf{v}_2$, $\mathbf{v}_5$ and $\mathbf{v}_6$ shown in figure 5 are the extreme lines of sight to have crossings between the two curve segments

The vectors $\mathbf{t}$, $\mathbf{u}$ and $\mathbf{t}\times\mathbf{u}$ forms a moving frame along the curve $\mathbf{K}$ which is similar to Frenet frame. The vector $\frac{d\mathbf{u}}{ds}$ measures how the curve $\mathbf{L}$ is moving with respect to curve $\mathbf{K}$. Taking the dot product with $\mathbf{t}\times\mathbf{u}$ measures how much it is moving in a direction perpendicular to the direction of the curve.

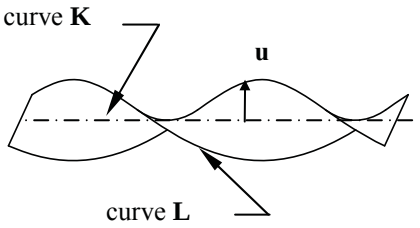

(a) A ribbon

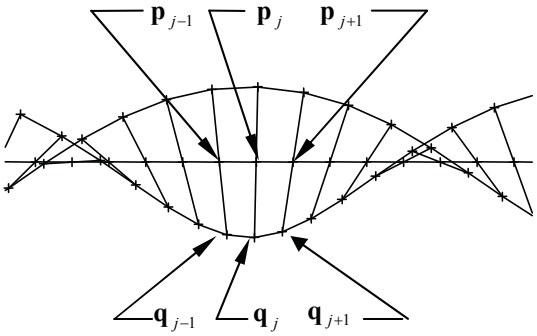

(b) A discrete ribbon model

Figure 4: A ribbon and its model

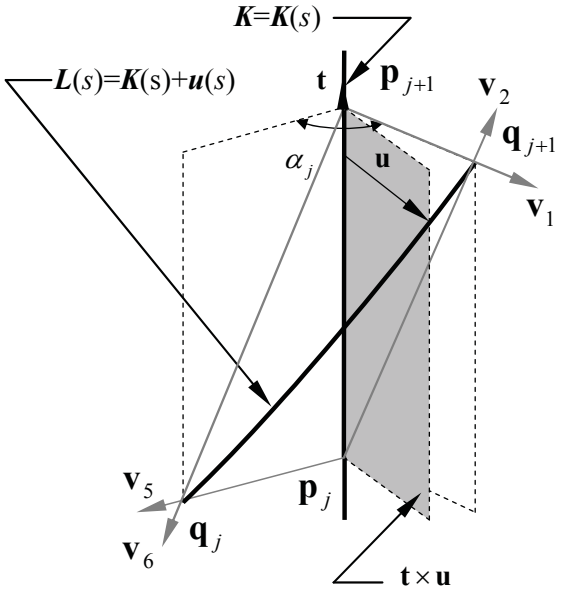

Figure 5: Segment on curve $\mathbf{L}$ twists around segment on curve $\mathbf{K}$

3.2 Equations and mathematical expressions

The crossing map of segment $\mathbf{q}_j\ \mathbf{q}_{j+1}$ with respect to segment $\mathbf{p}_j\ \mathbf{p}_{j+1}$ is shown in figure 6. Since curve $\mathbf{K}$ and $\mathbf{L}$ have the relationship $\mathbf{L}(s) = \mathbf{K}(s) + \mathbf{u}(s)$, the crossing map $\chi_K(\mathbf{u})$ is a portion of equator with dihedral angle α_j. The spherical region $\mathbf{v}_1\mathbf{v}_2\mathbf{v}_5\mathbf{v}_6$ is the crossing map $\chi_K(\mathbf{pq})$ with points $\mathbf{p}$ and $\mathbf{q}$ on segment $\mathbf{p}_j\ \mathbf{p}_{j+1}$ and segment $\mathbf{q}_j\ \mathbf{q}_{j+1}$ respectively. Due to the twist condition, the crossing maps are within the spherical lune with dihedral angle α_j.

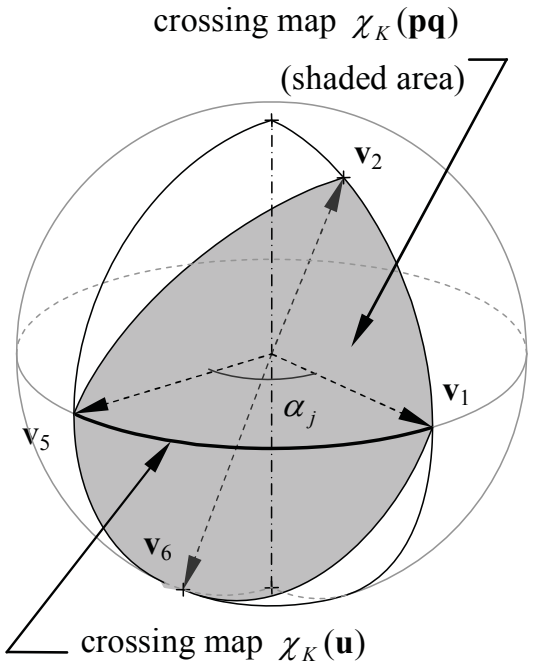

Figure 6: Crossing maps of segments $\mathbf{p}_j\ \mathbf{p}_{j+1}$ and $\mathbf{q}_j\ \mathbf{q}_{j+1}$

A parameter t ($t \in [0,1] \subset R$) is used to characterize the material between the curves. The material between curve $\mathbf{K}$ and $\mathbf{L}$ is expressed as curve $\mathbf{M}$ on the ribbon parallel to $\mathbf{K}$ and $\mathbf{L}$ with a specific parameter t:

$$\mathbf{M}(s) = (1-t)\mathbf{K}(s) + t \cdot \mathbf{L}(s), \quad \forall s \in R,\ 0 \le t \le 1 \tag{13}$$

When t = 1, curve $\mathbf{M}$ coincides with curve $\mathbf{L}$ which implies no material is between the curves $\mathbf{K}$ and $\mathbf{L}$.

Let $\mathbf{M}$ be the series of line segments $M = \mathbf{r}_1\mathbf{r}_2\cdots\mathbf{r}_n$. The spherical quadrilateral $\mathbf{v}_1\mathbf{v}_2\mathbf{v}_5\mathbf{v}_6$ is defined as

$$\mathbf{v}_1\mathbf{v}_2\mathbf{v}_5\mathbf{v}_6 = \Big\{\mathbf{v}|\mathbf{v} = \chi_K(\mathbf{pr}), \quad \forall \mathbf{p} \in \mathbf{K},\ \mathbf{r} \in \mathbf{M} = \mathbf{L}\Big\} \tag{14}$$

Figure 7 depicts the crossing map with $1 > t > 0$. The shaded region within the spherical lune is the accumulated crossing map with respect to curve $\mathbf{K}$ as the parameter t decreases from 1. As the parameter t starts changing from 1, the location of curve $\mathbf{M}$ slides away from curve $\mathbf{L}$ and moves towards curve $\mathbf{K}$. This is equivalent to thickening curve $\mathbf{L}$ (or adding material between curves $\mathbf{L}$ and $\mathbf{M}$) as parameter t decreases from 1. In figure 7(a), the shaded region $\mathbf{v}_1\mathbf{v}_2\mathbf{v}_5\mathbf{v}_6$ (as shown in figure 5) is enlarged to $\mathbf{v}_1\mathbf{v}_3\mathbf{v}_5\mathbf{v}_7$ as the parameter t decreases from 1 to 0.5. This is the accumulated crossing map of the "thickened" curve segments $\mathbf{L}$ (with width t) with respect to curve segment $\mathbf{K}$,

$$\mathbf{v}_1\mathbf{v}_3\mathbf{v}_5\mathbf{v}_7 = \bigcup\nolimits_{t,1\ge t>0.5} \Big\{\mathbf{v}|\mathbf{v} = \chi_K(\mathbf{pr}), \quad \forall \mathbf{p} \in \mathbf{K},\ \mathbf{r} \in \mathbf{M} = (1-t)\mathbf{K} + t \cdot \mathbf{L}\Big\} \tag{15}$$

Hence, the complete spherical lune $\mathbf{v}_1\mathbf{v}_4\mathbf{v}_5\mathbf{v}_8$ is the crossing map of a ribbon with spine curve $\mathbf{K}$ and boundary curve $\mathbf{L}$

$$\mathbf{v}_1\mathbf{v}_4\mathbf{v}_5\mathbf{v}_8 = \bigcup\nolimits_{t,1\ge t\ge 0} \Big\{\mathbf{v}|\mathbf{v} = \chi_K(\mathbf{pr}), \quad \forall \mathbf{p} \in \mathbf{K},\ \mathbf{r} \in \mathbf{M} = (1-t)\mathbf{K} + t \cdot \mathbf{L}\Big\} \tag{16}$$

The twist Tw_j between segment $\mathbf{p}_j\ \mathbf{p}_{j+1}$ and segment $\mathbf{q}_j\ \mathbf{q}_{j+1}$ is the average crossing over every possible line of sight, hence

$$Tw_j = \frac{\Omega_j}{4\pi} \tag{17}$$

From equation (4), the solid angle is area of the spherical lune which is $2\alpha_j$, hence,

$$Tw_j = \frac{\alpha_j}{2\pi} \tag{18}$$

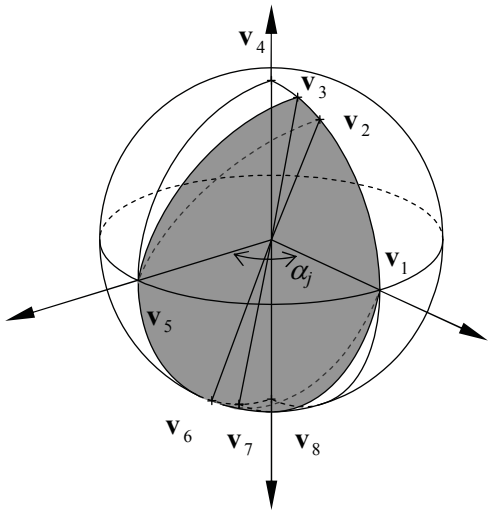

(a) Crossing map of the thickened curve **L** (as t decreases from 1 to 0.5) with respect to curve **K**.

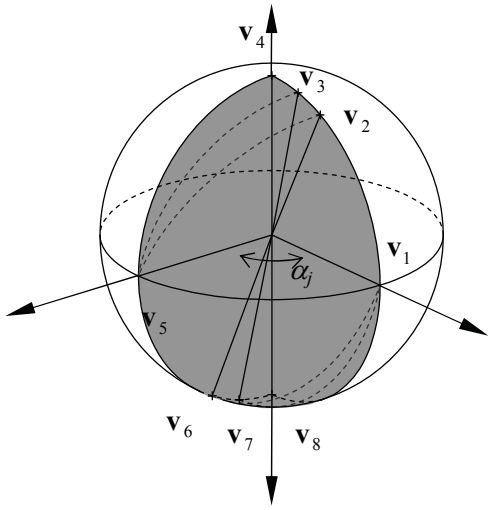

(b) Crossing map of the thickened curve **L** (as t decreases from 0.5 to 0) with respect to curve **K**.

Figure 7: The crossing maps of a twisted ribbon

Hence, the twist of a ribbon is

$$Tw(\mathbf{K},\mathbf{L}) = \frac{1}{2\pi}\sum_{j=1}^{n}\alpha_j \tag{19}$$

where

$$\alpha_j = \cos^{-1}\left(\frac{\mathbf{q}_j\mathbf{p}_j\times\mathbf{q}_j\mathbf{p}_{j+1}}{\left\|\mathbf{q}_j\mathbf{p}_j\times\mathbf{q}_j\mathbf{p}_{j+1}\right\|}\cdot\frac{\mathbf{q}_{j+1}\mathbf{p}_j\times\mathbf{q}_{j+1}\mathbf{p}_{j+1}}{\left\|\mathbf{q}_{j+1}\mathbf{p}_j\times\mathbf{q}_{j+1}\mathbf{p}_{j+1}\right\|}\right)$$

$\forall\mathbf{p}_j\in\mathbf{K}$ and $\forall\mathbf{q}_j\in\mathbf{L}$.

Figure 8 shows two examples of computing the twist and writhe of two conformations of an open end ribbon by considering the area of the crossing maps. In figure 8(a), a twisted ribbon and its discrete model with six segments are shown. Hence, there are six lunes (cyan region) on the unit sphere as the crossing map. Similarly, a discrete coiled ribbon of ten segments is employed to depict the crossing map in figure 8(b). The crossing map consists of two parts; one is on the left hand side of the northern hemisphere which the other part is on the right hand side of the southern hemisphere. For these two simple conformations, a point in the map refers to a line of sight from the centre of the unit sphere to the point which gives one crossing (the map shown in figure 8(a) gives a crossing between curves **K** and **L** while that in figure 8(b) yields a self crossing of curve **K**).

4 Călugăreanu's theorem

The mathematics of knot theory for which Călugăreanu's theorem is one of the pillars applying to closed end curves. It relates the linking number (the topology) with the writhe and twist (the geometry) of a ribbon model. The linking number of a closed end ribbon is an invariant while writhe and twist are interchangeable. Mathematically,

$$Lk(\mathbf{K},\mathbf{L}) = Wr(\mathbf{K},\mathbf{K}) + Tw(\mathbf{K},\mathbf{L}) \tag{20}$$

4.1 Algebraic property

Since curves **K** and **L** are closed end, their crossing maps cover the entire unit sphere. Hence the expression $\sum_{\substack{j=1,\\ n+1=1}}^{n}\sum_{\substack{k=1,\\ n+1=1}}^{n} S_{jk}^{Lk}$ covers the whole unit sphere. The linking number is obtained by dividing it by the area of the unit sphere surface (which is 4π). Hence, the linking number of two closed end curves is an integer number of times that the unit sphere covered by the image of the two curves under the mapping χ_K. On the other hand, the geometry of a ribbon is described by its writhe and twist. Summing up the writhe (Wr) and twist (Tw), which are not necessarily integers (indeed most often they are real numbers), *always* yields an integer (linking number Lk).

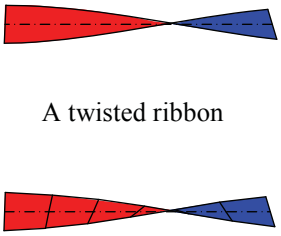

A twisted ribbon

A discrete twisted ribbon

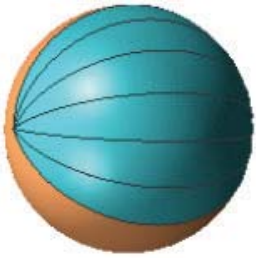

Crossing map

(a) A twisted ribbon and its crossing map

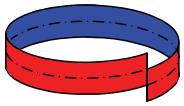

A coiled ribbon

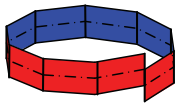

A discrete coiled ribbon

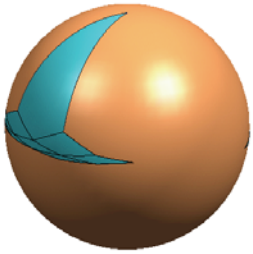

Crossing map

(b) A coiled ribbon and its crossing map

Figure 8: Discrete ribbon models and their crossing maps

It is obvious to explain the reason by considering their geometric interpretations.

Substituting equation (8), (10) and (19) into equation (20) yields

$$S_{total} = S_{Wr} + S_{Tw} \tag{21}$$

where $S_{total} = \sum_{\substack{j=1,\\ n+1=1}}^{n} \sum_{\substack{k=1,\\ n+1=1}}^{n} S_{jk}^{Lk} \in R$ is the total area of the crossing maps on the unit sphere, $S_{Wr} = \sum_{\substack{j=1\\ j\neq k\\ j\neq k\pm 1\\ n+1=1}}^{n} \sum_{\substack{k=1\\ n+1=1}}^{n} S_{jk}^{Wr} \in R$ is the area of the crossing maps due to the writhe and $S_{Tw} = 2\sum_{j=1}^{n} \alpha_j \in R$ is the area of the crossing maps due to the twist.

Rewriting equation (21) as

$$Lk(\mathbf{K},\mathbf{L}) \cdot 4\pi = S_{Wr} + S_{Tw} \tag{22}$$

The three quantities $Lk(\mathbf{K},\mathbf{L}) \cdot 4\pi$, S_{Wr} and S_{Tw} are all real numbers. Rearranging yields

$$Lk(\mathbf{K},\mathbf{L}) = \frac{S_{Wr}}{4\pi} + \frac{S_{Tw}}{4\pi} \tag{23}$$

Therefore, the two geometric quantities $\frac{S_{Wr}}{4\pi}$ (which is Wr) and $\frac{S_{Tw}}{4\pi}$ (which is Tw) on the right hand side of equation (20) are real numbers and the topological quantity $Lk(\mathbf{K},\mathbf{L})$ on the left is an integer.

4.2 Open end ribbon

Whatever the linking number between two closed end curves might be, the change in the geometry as writhe and twist counter-balances each other. Algebraically, the derivative of a constant (for the linking number) is zero. Therefore, according to (20)

$$\delta Wr(\mathbf{K},\mathbf{K}) + \delta Tw(\mathbf{K},\mathbf{L}) = 0 \tag{24}$$

When a system is closed, as in the case of a knot (or with the total energy in a system), there tends to be a "conservation" theorem characterizing the behavior of the different aspects in the closed system. Yet, most proteins in their native forms are open end. To save Călugăreanu's theorem, the notion of "nano-robotics" comes to rescue.

The mechanics of a single bio-molecule at the nanometer scale is an important pursuit as it provides insight into how a molecule functions under external influences, as well as in revealing the limitations of classical mechanics in the Newtonian scale. The forces underlie the various chemistries and molecular biology of genetic material are of the order of μN. Several techniques differing in force ranges are available: atomic force microscopy [Mehta, Rief, Spudich, Smith and Simmons (1999)](AFM), optical tweezers, and magnetic tweezers [Fritz, Baller, Lang, Rothuizen, Vettiger, Meyer, Güntherodt, Gerber and Gimzewski (2000), Eggar (2000)]. Mechanicstically, a molecule is "clamped" at one end and on a substrate and is manipulated by the other, free end. Both the AFM and optical tweezers are for applying pulling forces on the free end, in different force ranges. The forces range for

AFM is greater than 1μN while that for the optical tweezers is between 0.1μN to 150μN. Measuring the rate and force at which a DNA is packed by a virus is an example of using the optical tweezers. Pulling or pushing is translational. If rotational input is required, such as in coiling a DNA and measuring the rate of uncoiling by an enzyme, the magnetic tweezers are used. The typical force range for a magnetic tweezer is 0.01-100μN. In geometry, these nano-manipulation apparatuses effectively close the open end curve.

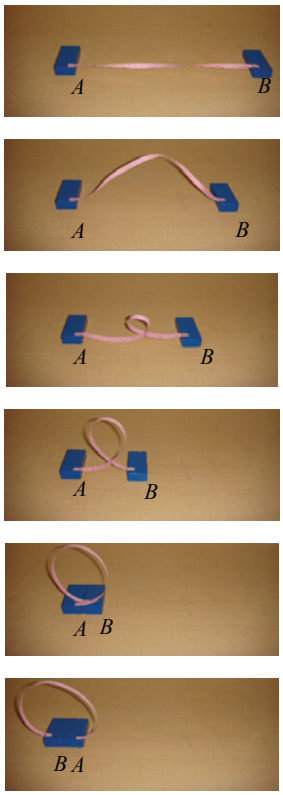

(a) Twisting an open end ribbon by 2π.

(b) End B of the ribbon moves toward end A which is fixed.

(c) Supercoiling conformation forms.

(d) Another supercoiling conformation as one end gets closer to the other end.

(e) Another supercoiling conformation as both ends meet.

(f) End B moves to the "other" side of end A.

Figure 9: Various conformations due to the motion of the ribbon ends

Twisting an open end ribbon by 2π as depicted in figure 9(a) yields a conformation with planar central spine **K**. The self crossing map of this curve on the unit sphere is a great circle with zero area. Hence, the writhe of a twisted ribbon is zero and the twist is 1. As one end of the ribbon moves towards the other end, the twisted ribbon turns into a coiled ribbon as shown in figure 9(b) – 9(e).

Twenty points are marked on the spline **K** and boundary curve **L** of a ribbon respectively and their spatial positions in each shown conformation are measured. Three canonical conformations of the ribbon are illustrated in figure 10. Figure 10(a) shows a twisted ribbon while a coiled ribbon is shown in figure 10(b) and 10(c). Their writhe and twist are computed.

The writhe (Wr) and twist (Tw) of the conformations shown in figure 10(a) and 10(b) conforms to equation (24). However, the conformation shown in figure 10(c) (which is the same the conformation shown in figure 9(f)) yields a decrement in writhe (a) A twisted ribbon with Wr=0, Tw=1 as shown in figure 9(a).

A coiled ribbon with $Wr \cong 0.95$, $Tw \cong 0.05$ as shown in figure 9(e).

Another conformation of a coiled ribbon with $Wr \cong 0.07$, $Tw \cong 0.05$ as shown in figure 9(f).

(a) A twisted ribbon with Wr=0, Tw=1 as shown in figure 9(a)

(b) A coiled ribbon with $Wr \cong 0.95$, $Tw \cong 0.05$ as shown in figure 9(e)

(c) Another conformation of a coiled ribbon with $Wr \cong 0.07$, $Tw \cong 0.05$ as shown in figure 9(f)

Figure 10: Canonical ribbon conformations

When the ends of an open end ribbon is held (for instance, the DNA or protein molecules held by the nano-manipulation apparatuses), it is equivalent to have an imaginary ribbon connecting both ends as illustrated in figure 11. A twisted open end ribbon is shown on the left hand side with two ends A and B. As end B of the ribbon moves to-

wards end A, it turns into a coiled ribbon as shown on the right hand side with the twist converting into writhe.

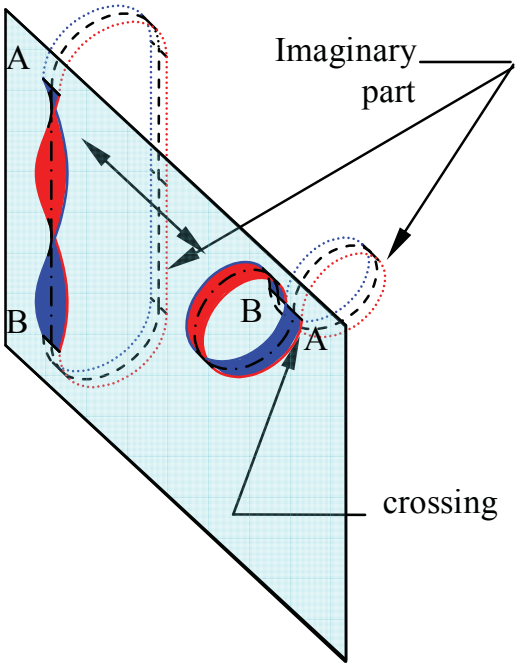

Figure 11: Closing an open end ribbon

Rewriting the closed end curve $\mathbf{K} = \mathbf{K}_r \cup \mathbf{K}_i$ and $\mathbf{L} = \mathbf{L}_r \cup \mathbf{L}_i$ where the subscripts r and i represent the real part and the imaginary part of a "closed" end ribbon respectively. The writhe $Wr(\mathbf{K},\mathbf{K})$ and the twist $Tw(\mathbf{K},\mathbf{L})$ are expressed as

$$Wr(\mathbf{K},\mathbf{K}) = Wr(Wr(\mathbf{K}_r,\mathbf{K}_r)) + Wr(Wr(\mathbf{K}_i,\mathbf{K}_i)) + 2Wr(Wr(\mathbf{K}_i,\mathbf{K}_r)) \quad (25)$$

where

$$Wr(Wr(\mathbf{K}_r,\mathbf{K}_r)) = \frac{1}{4\pi}\sum_j\sum_k S^{Wr}_{jk}, \quad \forall \mathbf{p}_j \in \mathbf{K}_r, \mathbf{q}_j \in \mathbf{K}_r$$

;

$$Wr(Wr(\mathbf{K}_i,\mathbf{K}_i)) = \frac{1}{4\pi}\sum_j\sum_k S^{Wr}_{jk}, \quad \forall \mathbf{p}_j \in \mathbf{K}_i, \mathbf{q}_j \in \mathbf{K}_i$$

and

$$Wr(Wr(\mathbf{K}_i,\mathbf{K}_r)) = \frac{1}{4\pi}\sum_j\sum_k S^{Wr}_{jk} = Wr(\mathbf{K}_r,\mathbf{K}_i) \quad \forall \mathbf{p}_j \in \mathbf{K}_r, \mathbf{q}_j \in \mathbf{K}_i$$

$$Tw(\mathbf{K},\mathbf{L}) = Tw(Wr(\mathbf{K}_r,\mathbf{L}_r)) + Tw(Wr(\mathbf{K}_i,\mathbf{L}_i)) \quad (26)$$

where

$$Tw(Wr(\mathbf{K}_r,\mathbf{L}_r)) = \frac{1}{2\pi}\sum_j \alpha_j, \quad \forall \mathbf{p}_j \in \mathbf{K}_r \text{ and } \forall \mathbf{q}_j \in \mathbf{K}_r$$

and

$$Tw(Wr(\mathbf{K}_i,\mathbf{L}_i)) = \frac{1}{2\pi}\sum_j \alpha_j, \quad \forall \mathbf{p}_j \in \mathbf{K}_i \text{ and } \forall \mathbf{q}_j \in \mathbf{K}_i$$

Therefore, substituting equation (25) and (26) into (24) and rearranging yields

$$\underbrace{\delta Wr(Wr(\mathbf{K}_r,\mathbf{K}_r)) + \delta Tw(Wr(\mathbf{K}_r,\mathbf{L}_r))}_{\text{real part of the ribbon}} + \underbrace{\delta Wr(Wr(\mathbf{K}_i,\mathbf{K}_i)) + \delta Tw(Wr(\mathbf{K}_i,\mathbf{L}_i)) + 2\delta Wr(Wr(\mathbf{K}_i,\mathbf{K}_r))}_{\text{Imaginary part of the ribbon}} = 0 \quad (27)$$

Equation (27) can be categorized into two parts, the real part (which is equivalent to an open end ribbon) and the imaginary part of a "closed" end ribbon.

When an open end ribbon is isotropic to a new conformation, any change in twist will be exactly balanced by the change in its writhe provided the crossings due to either twist or writhe remain in the real part as shown in figure 8(a)-8(e). This condition refers to $\delta Wr(Wr(\mathbf{K}_i,\mathbf{K}_i)) = 0$, $\delta Wr(Wr(\mathbf{K}_i,\mathbf{K}_r)) = 0$ and $\delta Tw(Wr(\mathbf{K}_i,\mathbf{L}_i)) = 0$ in equation (27) which gives

$$\delta Wr(Wr(\mathbf{K}_r,\mathbf{K}_r)) + \delta Tw(Wr(\mathbf{K}_r,\mathbf{L}_r)) = 0 \quad (28)$$

When the crossings (due to either twist or writhe) are moved to the imaginary part as shown in figure 8(f), the terms $\delta Wr(Wr(\mathbf{K}_i,\mathbf{K}_i))$, $\delta Wr(Wr(\mathbf{K}_i,\mathbf{K}_r))$ and $\delta Tw(Wr(\mathbf{K}_i,\mathbf{L}_i))$ no longer vanish and the changes in twist and writhe in the open end (the real part) ribbon do not counter balance each other. Hence, the writhe decreases as the crossing moves to the imaginary part.

5 Concluding remarks

The geometry and the topology of a ribbon are related to each other by their linking number, writhe and twist. It turns out that these three quantities in the Călugăreanu's theorem are rooted in the notion of an area on a unit sphere, more generally known as the *Gauss Integral*. Behind these quantities are the crossings. The integrals can be very complicated and are hard to compute for a complex ribbon conformation, since no analytic expression is available for the curves. Simplification is offered by having considered their geometric interpretations. These geometric interpretations also reveal the reason for the property of the Călugăreanu's theorem that adding two real numbers (writhe Wr and twist Tw) always yields an integer (linking number Lk). The change in twist and writhe for an open end ribbon is also discussed.

The Călugăreanu's theorem accounts for the transformation between a twisted ribbon and a coiled ribbon which happens in many biological processes. To understand these processes better, many more issues deserve further exploration – one of which has to the forces and energies that drive a molecule from one conformation to another.

6 References

Agarwal, P. K.; Edelsbrunner, H.; Wang, Y. (2002): Computing the writhing number of a polygonal knot. *Discrete & Computational Geometry*, Vol.32, No.1, pp.37-53.

Banchoff, T. (1976): Self linking numbers of space polygons. *Indiana University Mathematical Journal*, vol.25, no.12, pp.1171-1188.

Călugăreanu, G. (1959): L'intégrale de Gauss et l'Analyse des nœuds tridimensionnels. *Revue Roumaine de Mathématiques Pures et Appliquées*, Vol.4, pp.5-20.

Carson, M.; Bugg, C. E. (1986): Algorithm for ribbon models of proteins. *Journal of Molecular Graphics*, vol.4, no.2, pp.121-122.

Carson, M.; Bugg, C. E. (1987): Ribbon models of macromolecules. *Journal of Molecular Graphics*. Vol.5, no.2, pp.103-106.

Carson, M.; Bugg, C. E. (2000): Early ribbon drawings of proteins. *Natural Structural and Molecular Biology*, vol.7, no.8, pp.624-625.

Cimasoni, D. (2001): Computing the writhe of a knot. Journal of Knot Theory Ramifications, vol.10, pp.387-295.

Cozarelli, N. R.; Boles, T.; White, J. (1990): DNA Topology and its biological effects, Cold Spring Harbor Laboratory Press.

Dennis, M. R.; Hannay, J. H. (2005): Geometry of Călugăreanu's Theorem. *Proceedings of the Royal Society A: Mathematical Physical and Engineering Sciences*, vol.461, no.2062. pp.3245-3254.

Eggar, M. H. (2000): On White's formula. *Journal of Knot Theory and its Ramification*, vol.9, no.5, pp.611-615.

Fritz, J.; Baller, M. K.; Lang, H. P.; Rothuizen, H.; Vettiger, P.; Meyer, E.; Güntherodt, H. J.; Gerber, C. H.; Gimzewski, J. K. (2000): Translating biomolecular recognition into nanomechanics. *Science*, vol.288, no.5464. pp.316-318.

Fuller, F. B. (1971): The writhing number of a space curve. *Proceedings of the National Academy of Science*, vol.68, pp.815-819.

Karcher, H.; Lee, S. E.;Kaazempur-Mofrad, M. R.; Kamm, R. D. (2006): A coarse-grained model for force-induced protein deformation and kinetics. *Biophysical Journal,* vol. 90, no.8, pp.2686-2697.

Klenin, K.; Langowski, J. (2000): Computation of writhe in modeling of supercoiled DNA. *Biopolymers*, vol.54, pp.307-317.

Mehta, A. D.; Rief, M.; Spudich, J. A.; Smith, D. A.; Simmons R. M. (1999):Single-molecule biomechanics with optical methods. *Science*, vol.283, no. 5408, pp.1689-1695.

Park, J. Y.; Cho, Y. S.; Kim, S. Y.; Jun, S.; Im, S. (2006): A quasicontinuum method for deformations of carbon nanotubes. *CMES: Computer Modeling in Engineering & Science*, Vol.11, no.2, pp.61-72.

Steffen N. R.; Murphy, S. D.; Lathrop, R. H.; Opel, M. L.; Tolleri, L.; Hatfield, G. W. (2002):

The role of DNA deformation energy at individual base steps for the identification of DNA-protein binding sites. *Genome Informatics*, vol. 13, pp. 53-162.